Journal of Power Sources 195 (2010) 7517–7523

Contents lists available at ScienceDirect

Journal of Power Sources

journal homepage: www.elsevier.com/locate/jpowsour

Studies on metal hydride electrodes containing no binder additives

Z. Rogulski[b,*], J. Dłubak[b], M. Karwowska[a], M. Krebs[c], E. Pytlik[c], M. Schmalz[c], A. Gumkowska[a], A. Czerwiński[a]

[a] Department of Chemistry, Warsaw University, Pasteura 1, 02-093 Warsaw, Poland
[b] Industrial Chemistry Research Institute, Rydygiera 8, 01-793 Warsaw, Poland
[c] VARTA Microbattery GmbH, Daimlerstraße 1, 73479 Ellwangen, Germany

ARTICLE INFO

Article history:
Received 15 September 2009
Accepted 12 December 2009
Available online 21 December 2009

Keywords:
Ni-MH battery
Hydrogen sorption
Diffusion coefficient
Limited Volume Electrode
AB_5 alloy

ABSTRACT

Electrochemical properties of hydrogen storage alloys (AB_5 type: LaMm-$Ni_{4.1}Al_{0.3}Mn_{0.4}Co_{0.45}$) were studied in 6 M KOHaq using Limited Volume Electrode (LVE) method. Working electrodes were prepared by pressing alloy powder (without binding and conducting additives) into a metal net wire serving as a support and as a current collector. Cyclic voltammetry curves reveal well defined hydrogen sorption and desorption peaks which are separated from other faradic processes, such as surface oxidation. Voltammograms of LVE resemble the curves obtained by various authors for single particle metal alloy electrodes. Hydrogen diffusion coefficient calculated at room temperature for LV electrodes and for 100% state of charge reaches a constant value of ca. 3.3×10^{-9} and 2.1×10^{-10} $cm^2\ s^{-1}$, for chronoamperometric and chronopotentiometric measurements, respectively. A comparison of the electrodes with average alloy particle sizes of ca. 50 and 4 μm allows us to conclude that at room temperature hydrogen storage capability of AB_5 alloy studied is independent on the alloy particle size. On the other hand, reduction of the particle size increases alloy capacity at temperatures below −10 °C and reduces time of electrochemical activation of the electrode.

1. Introduction

The nickel-metal hydride (Ni-MH) and Lithium Ion/Polymer batteries represent one of the most important segments of modern battery market. Although excellent for powering of many of portable devices or Hybrid Electro Vehicles (HEV) [1–3], the attainable current densities of these batteries are not sufficient for the use in devices in low temperature or requiring very high power densities, like e.g. power-tools. This limitation prohibits effective replacement of containing toxic elements Ni–Cd batteries in nearly all segments of the battery market.

It is well established that the weight of the materials used for battery construction reduces the theoretical energy density, even by a factor of two. As a consequence, the actual energy that is available from a battery under practical, close to optimum, discharge conditions constitutes only about 30% of the theoretical energy of the active materials [1]. Thus, new electroactive materials are under development and the construction of batteries is modified in order to improve their energy efficiency. Such a development, however, requires considerations of various factors that have significant influence on the electrode performance. In the case of nickel-metal hydride battery these factors include: the electrode configuration, the active material porosity and the thickness, the alloy composition, the alloy particle size and structure and the electrolyte composition [4–13].

A huge variety of metal hydride materials has been examined for application in NiMH batteries. Some of them cannot be applied in industrial scale due to high hydrogen equilibrium pressure at room temperature or instability when in contact with the electrolyte [14–17]. Investigation of a new hydrogen storage material, such as thin films of magnesium based alloys, requires optimization of the procedure of the electrode preparation. Typically, the metal hydride electrodes for electrochemical tests are prepared by mixing and pressing of a hydrogen storage alloy powder together with a binding material, e.g., PTFE, PVA, graphite, or metal powders [1,5,7–9]. The binding material absorbs the forces generated due to volume expansion during charging of alloy particles and, thereby, helps preserving the mechanical integrity of the electrode. The metallic and carbon additives also improve the overall electronic conductivity of the electrode. The presence of the additives, however, has a significant influence on the electrode resistance and stability of hydrogen inside the alloy. When a new material for a metal alloy hydride electrode is tested, the intrinsic electrochemical properties of hydrogen absorbing alloy are the first to be determined. This task requires preparation of a new type of electrode containing only the alloy studied and free of binding

* Corresponding author. Tel.: +48 22 5682447.
E-mail address: zbigniew.rogulski@ichp.pl (Z. Rogulski).

0378-7753/$ – see front matter © 2009 Elsevier B.V. All rights reserved.
doi:10.1016/j.jpowsour.2009.12.050

materials. The electrodes especially useful for studying bulk electrode processes, such as hydrogen sorption, are Limited Volume Electrodes, LVE, already applied in our previous studies of hydrogen absorption in metals and alloys [18–20]. The Limited Volume Electrode (LVE) is an electrode containing a thin layer of a hydrogen storage material attached, e.g. by electrochemical deposition, to a matrix which is neutral in respect to hydrogen absorption processes and acts as a current collector [18–20]. Cyclic voltammetry is the method excellently showing advantages of application of LVE. Voltammograms of bulk hydrogen absorbing materials, such as Pd wires or foils, are dominated by high currents due to hydrogen absorption and its subsequent oxidative removal [18]. The oxidation of a large amount of hydrogen dissolved in the bulk of the metal occurs slowly due to diffusional limitations. This resulted in overlapping of currents of hydrogen desorption and surface oxidation. Under such conditions the surface oxides reduction peak is poorly defined and separation of surface oxidation currents from the currents of oxidative hydrogen desorption is practically impossible [18]. On the contrary, potentiodynamic desorption of hydrogen absorbed in a Pd-LVE is faster and takes place in a narrow potential range being completed well before the onset potential of the surface oxidation. Thus, the use of LVEs results in cyclic voltammetry curves with well separated signals of hydrogen absorption/desorption and surface oxidation/oxides reduction currents and being of comparable magnitude [18]. Moreover, formation of a very thin layer of MH alloy particles in a LV electrode allows omission of binding materials which are essential in construction of thicker MH alloy electrodes. Thus, Limited Volume Electrodes allow studying intrinsic electrochemical properties of the alloy particles without any influence of typical MH electrodes additives.

The aims of our works were: (i) preparation of thin electrodes (Limited Volume type) with various amounts of a metal hydride active material and without binder additives, (ii) determination of the stability of such prepared electrodes, (iii) evaluation of the electrochemical performance of the new metal-hydride electrodes and modified metal-hydride alloys.

2. Experimental

2.1. Limited Volume Electrode (LVE) preparation

Limited Volume type working electrodes were prepared by pressing a small amount (up to 22 mg) of an AB_5-type alloy (LaMm-$Ni_{4.1}Al_{0.3}Mn_{0.4}Co_{0.45}$) in an Au metal mesh (99.9%, Goodfellow) under pressure of up to 20 MPa. Two kinds of alloy materials with the above composition were investigated: the standard one with a mean particle size of ca. 50 μm (VARTA, Germany), and the modified one, developed in the HydroNanoPol project, with the particle size reduced to 2–6 μm. Au metal mesh served as a support for the alloy and as a current collector. The gold was selected as a matrix material due to: (i) high electrochemical and chemical stability; (ii) electrochemical neutrality with a wide potential window without faradic processes; (iii) neutrality in respect to hydrogen absorption processes; (iv) good electronic conductivity and (v) softness and compressibility allowing pressing of the alloy particles into the gold net without damaging the structure of the formers.

2.2. Electrochemical setup and techniques

All the electrochemical tests were performed in a three-electrode system in a Teflon cell. MH alloy pressed into a gold mesh was used as a working electrode, Hg|HgO|6 M KOH (HYDROMET, Poland) and a gold sheet (Mint of Poland) served as a reference and counter electrodes, respectively. All the potentials in the text are referred to Hg|HgO. LV-MH electrodes were placed in gold clamps acting as current collectors. The experiments with various depth of immersion of gold clamps proved that their contributions to the electrochemical signals measured was negligible. In some of the experiments, the LV-MH electrodes were placed in a Teflon holder with a design similar to the one used by Zheng et al. [4] and presented in Fig. 1.

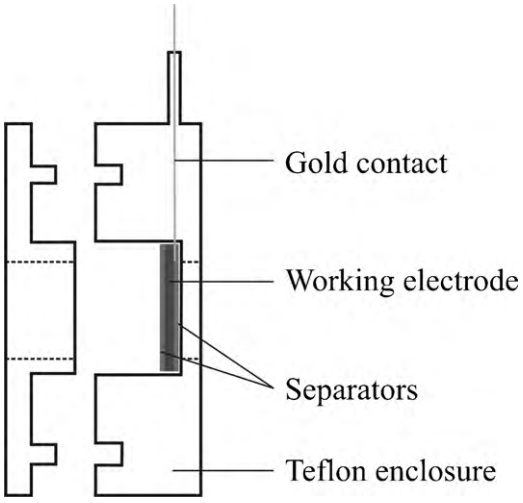

Fig. 1. Cross-section of Teflon holder containing limited volume type electrode.

The electrode was inserted between two pieces of a separator used in standard Ni-MH cell and a gold wire located between the electrode and one of separators acted as an electric contact. We found that such a design significantly reduces loss of the capacity of the MH-alloy electrode. The counter electrode was placed in a separated compartment and connected with the main cell compartment through a porous frit. The electrolyte solution of 6 M KOH was prepared with analytically grade reagents (POCh, Poland). Water used for preparation of solutions was subjected to two step purification procedure: double distillation as a first step and purification with Millipore system as a final step. The working solution was constantly deoxygenated with a small stream of pure argon (Multax, Poland) flowing through (before the measurements) and over the solution (during the measurements).

MH alloy electrodes were activated by 50 potential cycles in potential range between −1.1 and −0.4 V vs. Hg/HgO at 2 mV s^{-1} and subsequent three cycles of constant-current charging at 60 mA g^{-1} and discharging at 45 mA g^{-1}. The voltammetric, chronoampeormetric and chronopotentiometric measurements were performed with an AUTOLAB 30 (Eco Chemie B.V., Netherlands) electrochemical analyzer. A scanning electron microscope LEO 435VP coupled with an EDS analyzer (Röntec EDR286) was used to analyze the structure and composition of the electrodes.

Low temperature measurements were carried out in Teflon cell described above and immersed in a KRYO51 bath in a Lauda (Proline 855) thermostat. The electrodes were fully charged at room temperature, and, after completing the charging process, temperature of the cell was lowered to the desired value in the range from −10 to −30 °C. This way, we were able to determine the influence of temperature on the process of the electrode discharge only.

3. Results

3.1. Physical characterisation of MH-alloy LV electrodes

Fig. 2 presents a SEM image of a freshly prepared working electrode. The image is combined with an EDS linear scan for Au shown on the bottom of the figure. We observe that the active alloy mass fills hollows of Au net with some uncovered parts of the net exposed

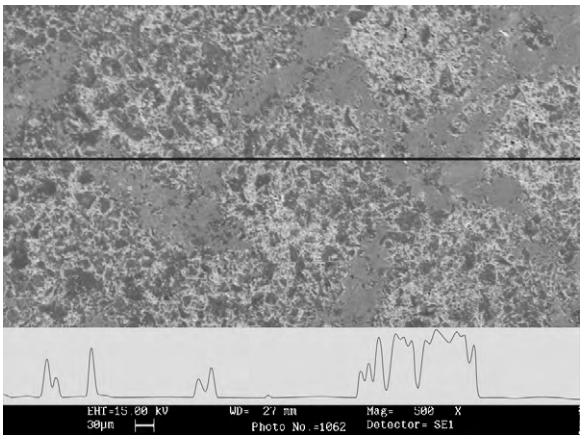

Fig. 2. SEM image and EDS linear analysis of a LV type electrode containing standard AB_5 alloy. EDS analysis for gold was performed along the line indicated on the image. Vertical scale of EDS spectrum is a net count number in arbitrary units. Magnification 500×.

to the ambient. The presence of uncovered Au was confirmed by EDS analysis showing an increase in Au net counts over the bare parts of Au wire net.

However, due to electrochemical neutrality of gold, this not affects results obtained for hydrogen absorption in MH alloy electrodes. As it will be discussed later, the only electrochemical contribution of gold is due to evolution of hydrogen during charging of the alloy.

An analysis of the electrode cross-section (Fig. 3) indicates the thickness of pressed alloy layer of ca. 50 μm. This value corresponds to the diameter of AB_5 alloy particles and indicates formation of an alloy layer with the thickness of a single particle. This way, ca. 25 000 single particles of hydrogen storage alloy are arranged in a single layer and each separate hole of gold matrix is filled by ca. 200–250 particles of the standard alloy. The borders between separate particles are well visible indicating that the particles do not form a bulk, continuous material and the process of hydrogen absorption/desorption in each of the particles proceeds independently. This way, hydrogen sorption/desorption in the electrodes studied may be treated as the one taking place in a particle with a spherical shape and under the conditions of a finite volume diffusion. In consequence, discussed type of Limited Volume Electrodes exhibits the electrochemical behaviour similar to that observed for single particle metal alloy electrodes [21]. This is one of main advantages of the electrode design presented.

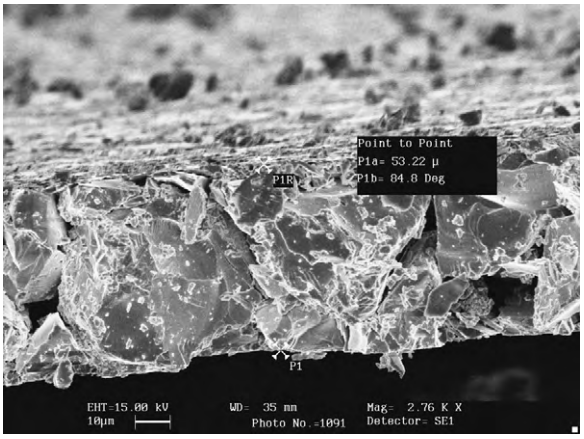

Fig. 3. SEM image of cross-section of LV type electrode containing standard AB_5 alloy. The distance between two points P1 and P1R is ca. 53 μm which corresponds to the diameter of a single standard alloy particle (ca. 50 μm). Magnification 2760×.

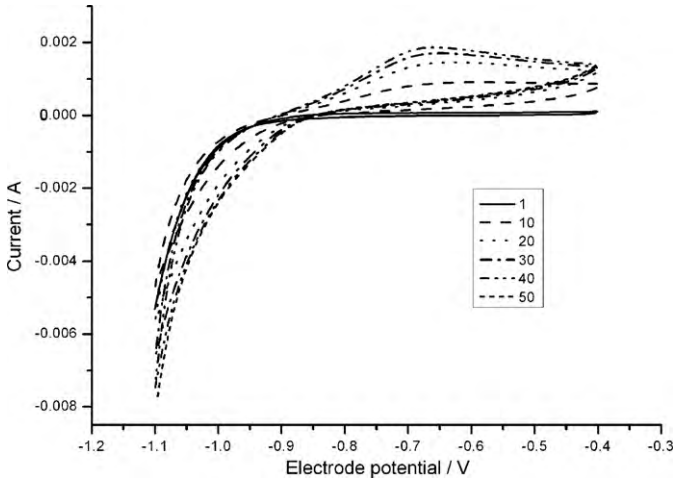

Fig. 4. Cyclic voltammetry curves of LVE type electrode containing standard AB_5 alloy. Alloy mass 14.6 mg, 6 M KOH, $v = 2\,mV\,s^{-1}$. Numbers denote number of CV cycle.

3.2. General cyclic voltammetry behaviour of Limited Volume MH-alloy electrodes

Fig. 4 shows cyclic voltammetry curves of a freshly prepared MH alloy electrode at various stages of potential cycling process. Positive limit of polarization (−400 mV) was selected as the one that ensures almost complete desorption of absorbed hydrogen and, simultaneously, as the one low enough as to prevent the electrode from irreversible oxidation (passivation), as judged from the electrochemical properties of Ni, the main component of the alloy.

Observed currents are attributed to oxidative hydrogen desorption (anodic peak with the top at ca. −0.75 V, well developed for advanced stages of the potential cycling process) and to hydrogen absorption with some contribution from hydrogen evolution process (cathodic currents starting at ca. −0.85 V). We note significant evolution of the shape of the voltammograms. The currents and charges due to hydrogen absorption and desorption increase with potential cycling time due to gradual increase in the electrode activity towards hydrogen uptake (Fig. 5).

Stabilisation of current profiles and charges of hydrogen absorption/desorption indicate attainment of a maximum activity of the

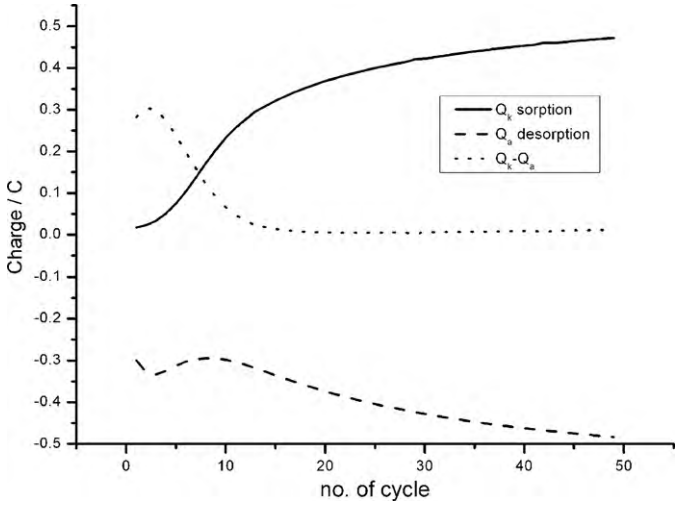

Fig. 5. The influence of the progress in potential cycling on the charges of hydrogen oxidation (Q_a) and reduction (Q_k) and their difference ($Q_k - Q_a$). Standard AB_5 alloy, 6 M KOH, potential scan rate $2\,mV\,s^{-1}$.

electrode (Fig. 5). Simultaneously, the difference between cathodic (absorption) and anodic (desorption) charges drops to almost zero. In this state full activation of the electrode material, surface activation and possibly also some bulk rearrangement is obtained. Time required for obtaining stable maximum activity depends on the alloy studied.

We have found that a decrease of the particle size of AB_5 alloy to 2–6 μm (a procedure developed in HydroNanoPol project) facilitates activation of the electrode by 20%. This effect can be attributed to the increase of the surface area of the alloy due to particle size reduction. Surface segregation of the alloy resulting from different procedures of particles preparation is another one factor which has to be taken into account. It is possible the surface of modified alloy is enriched with elements, e.g. nickel, facilitating hydrogen entry into the solid phase. A similar surface segregation in standard alloy can take place only during electrochemical activation which results in much longer time required for attainment of full electrode activity. Additionally, the specific packing of the alloy in the holes of gold mesh diminishes pulverisation of the alloy during the activation process.

In order to obtain as high state of charge as possible and for comparison with the results reported in the literature for single particle metal-hydride alloy electrodes [21], the small potential scan rates from 50 to 20 $\mu V\,s^{-1}$ were applied. Fig. 6 shows cyclic voltammograms obtained for a Limited Volume Electrode containing at least 25 000 alloy particles recorded at various scan rates.

As follows from Fig. 6, the electrode designed by us allows separation of hydrogen sorption and desorption currents from other faradic processes. The surface oxidation processes occurring at potentials higher than −650 mV have no significant influence on the shape of cyclic voltammograms. Moreover, similar to the single particle electrode, we observe well defined anodic peaks of hydrogen desorption and we can calculate the charge corresponding to hydrogen desorption [21]. For scan rates, v, lower than 50 $\mu V\,s^{-1}$ values of anodic current peak depend linearly on the square root of scan rate (see, inset to Fig. 6). Such a linear relation indicates that desorption is controlled by the process of hydrogen diffusion in alloy. For the scan rates higher than 50 $\mu V\,s^{-1}$ we observe a departure from the linearity on the anodic peak current vs. $v^{1/2}$ plot. One of the reasons of departure from linearity is the influence of the amount of absorbed hydrogen on the value of hydrogen diffusion coefficient, D, which is one of the parameters determining the slope of peak current vs. $v^{1/2}$ plots [22]. The amount of absorbed hydrogen

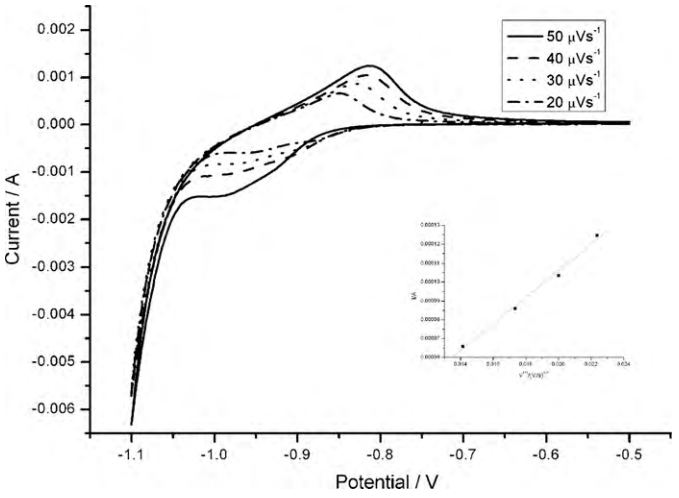

Fig. 6. Cyclic voltammetry curves of LV type electrode containing standard AB_5 alloy for various scan rates, v. Alloy mass 12.5 mg, 6 M KOH. The inset presents a relation between anodic peak current and $v^{1/2}$.

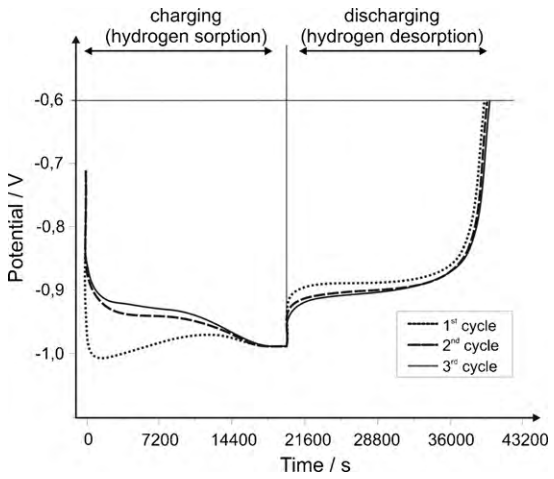

Fig. 7. Constant current charging (60 mA g^{-1}) and discharging (45 mA g^{-1}) of the Limited Volume Electrode containing standard AB_5 alloy. Shown are the curves for the first three cycles of charging/discharging.

depends on the potential scan rate so the changes in the scan rate affects also value of D. The relation between the amount of absorbed hydrogen an hydrogen diffusion coefficient will be discussed in subsequent chapter.

3.3. Hydrogen capacity and hydrogen diffusion coefficient in Limited Volume MH alloy electrodes

Two techniques were applied for determination of hydrogen diffusion coefficient; both of them were preceded by the activation process described in Section 2. In chronopotentiometric experiments (CP, Fig. 7) the absorption was performed with cathodic current equal to 60 mA g^{-1} and for time needed for charging of 125% of expected capacity. The charge of absorbed hydrogen was calculated on the basis of applied current and time needed for completing hydrogen charging process. The latter was evaluated on the basis of the shape of potential–time curves. After completing absorption process, desorption was accomplished with the current of 45 mA g^{-1} until potential of −600 mV was reached. Various states of charging of the electrode were obtained by varying hydrogen absorption time.

The practical specific hydrogen capacity obtained for standard and modified AB_5 alloys for 25 °C, and calculated for constant current discharging on the basis of transition time and applied desorption current, reach the values of 265 mAh g^{-1} ± 5% and 258 mAh g^{-1} ± 6%, respectively. These values are within the error range and correspond to ca. 85% of theoretical capacity reported by the manufacturer for the metal hydride alloy studied. This is in contrast to the results of other researcher who also investigated MH (AB_5) alloy particles with various sizes [7,9]. They reported that a decrease of the size of MH alloy particles below 25 μm reduces the specific discharging capacity of hydrogen storage material even by 40%.

Chronoamperometry (CA) was the second one technique applied for determination of hydrogen diffusion coefficient and the electrode capacity. In chronoamperometric experiments after initial short time polarization at potentials where no hydrogen absorption takes place (preconditioning), the electrode was first polarized at a potential of hydrogen absorption (−975 mV) for various time resulting in various values of *SOC*. After completing absorption process, the electrode was subjected to potential jump to the value where full desorption of hydrogen takes place (usually −600 mV). A comparison of anodic and cathodic charges indicates that the cathodic charges were slightly higher than anodic ones,

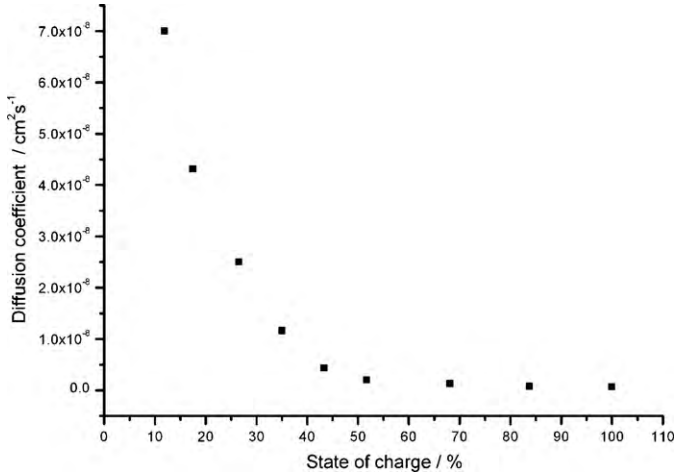

Fig. 8. Hydrogen diffusion coefficients of a LVE type electrode containing standard AB_5 alloy and calculated for constant current desorption (45 mA g^{-1}) as a function of the state of charge (*SOC*), T = 25 °C.

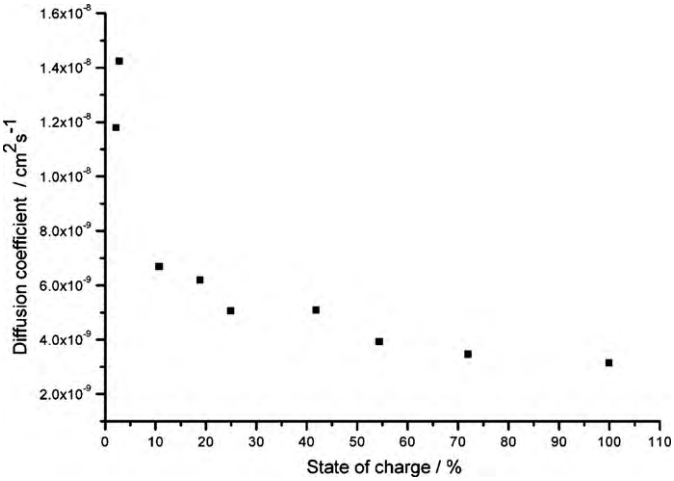

Fig. 9. Hydrogen diffusion coefficients in a standard AB_5 alloy calculated for constant potential desorption (−600 mV) as a function of the state of charge (*SOC*).

probably due to contribution of charges of hydrogen evolution. This would include charges of hydrogen evolution on bare parts of the metal net support.

The following equations were utilised for calculation of hydrogen diffusion coefficient, D:

- chronopotentiometric desorption was analyzed according to the model describing diffusion in a particle with a spherical symmetry [23]:

$$D = \frac{d^2}{15((Q_0/I) - \tau)} \quad (1)$$

where Q_0 is the initial hydrogen capacity (in charge units), τ is the transition time required for the hydrogen concentration on the surface to reach zero value, d is the radius of a single alloy particle (average value taken from SEM analysis and material technical specification delivered by manufacturer) and I is a constant current applied during discharging.

- the model of a finite space diffusion inside spherical particles [23] was applied in the analysis of chronoamperometric desorption curves:

$$I = \left(\frac{6FD(c_0 - c_s)}{\delta a^2}\right) \exp\left(\frac{-\pi^2 Dt}{d^2}\right) \quad (2)$$

where t is time, F is Faraday constant (96485 C mol^{-1}), δ the diffusion layer thickness, c_0 and c_s are bulk and surface hydrogen concentration, respectively, and the other terms have the same meanings as in Eq. (1). According to this equation, D can be calculated from the slope of a linear part of ln I vs. *time* plots. Because in our calculations we did not utilise the intercept of I vs. t plots (preexponential factor in Eq. (2)) the values of δ, c_0 and c_s have not to be determined.

Figs. 8 and 9 present diffusion coefficient values calculated from Eqs. (1) and (2) and presented as a function of the state of charge of the electrode, *SOC*.

In general, D values obtained by both techniques are very close and differ by less than 15%. We observe that for both techniques D decreases with an increase in *SOC* reaching a constant value for *SOC* > 50%. For *SOC* equal to 100% D values are 3.3×10^{-9} and 2.1×10^{-10} cm^2 s^{-1}, for CA and CP measurements, respectively. The influence of *SOC* on the value of hydrogen diffusion coefficient in various hydrogen absorbing materials is very often reported and discussed in the literature [23–25]. One of the explanations assumes that during diffusion hydrogen jumps between empty nearest-neighbour absorption sites (vacancies), in the direction determined by the concentration gradient. The occupation of these absorption sites by hydrogen increases when *SOC* increases. Hence, the higher the *SOC* the smaller the number of vacancies available for hydrogen transport and diffusion process is impeded [26]. Influence of *SOC* on D can be also attributed to hydrogen concentration dependent interactions between absorbed hydrogen or to a phase transition between various phases of alloy/metal-hydrogen systems and taking place when concentration of absorbed hydrogen increases [27,28]. Presented here D vs. *SOC* dependence can explain departure from linearity of presented in Fig. 6 plot of desorption current peak vs. $v^{1/2}$. In the case of cyclic voltammetry conditions, the various *SOC* values are realised by varying potential scan rate – the higher the scan rate the lower the *SOC* value due to shorter time of hydrogen absorption. On the other hand, according to Figs. 8 and 9, value of D increases with *SOC* decrease and for the higher values of scan rate the effective diffusion coefficient of hydrogen should be higher. Because in the process controlled by the rate of diffusion the peak current is directly proportional to D, the increase in the scan rate should shift the values of peak current above the straight line and this is observed in the inset to Fig. 6.

In order to confirm the correctness of application of presented equations, we performed an analysis of the influence of the mass of the alloy utilised in the electrode preparation on the calculated values of the diffusion coefficient (Fig. 10). As the figure shows, for fully charged electrode the diffusion coefficient does not depend on the mass of the alloy in the electrode. This observation confirms validity of a single spherical particle approach used in calculation of diffusion coefficient in Limited Volume Electrode configuration.

3.4. Modification of MH-alloy Limited Volume Electrode and comparison with standard types of MH electrode

The results obtained for MH-alloy LV electrode and prepared as described in Section 2 were compared with that obtained for a standard type MH electrodes. The latter were prepared according to Ni-MH battery manufacturer procedure, with addition of ca. 10% (w/w) of Ni powder acting as a conducting material. We also modified LVE setup by placing a LV electrode in a Teflon holder described in Section 2. Table 1 presents the values of diffusion coefficient and the capacity changes (normalized in respect to 3rd cycle of charging/discharging) for four tested electrodes: two of standard type with addition of Ni powder, a MH alloy LV electrode and for MH alloy LV electrode placed in a Teflon holder. As the table indicates,

Table 1
A comparison of electrochemical properties (diffusion coefficient and capacity stability) of AB_5 alloy electrodes containing various amounts of the alloy and Ni powder additives. Presented average values of diffusion coefficient, *D*, are for fully charged electrodes. Measurements for 25 °C, the capacity normalized in respect to 3rd cycle.

Electrode type	Capacity retention with life cycles of the electrodes, %			Average diffusion coefficient, $cm^2\ s^{-1}$	
	1st cycle	3rd cycle	20th cycle	CA	CP
Standard 1000 mg electrode containing 10% of Ni powder	96	100	89	7.1×10^{-9}	6.3×10^{-9}
Standard 100 mg electrode containing 10% of Ni powder	94	100	26	4.5×10^{-9}	2.3×10^{-9}
Limited Volume Electrode (17.2 mg of the standard alloy)	94	100	67	4.9×10^{-9}	8.1×10^{-9}
Limited Volume Electrode in a holder (15.3 mg of the standard alloy)	95	100	91	3.8×10^{-9}	5.8×10^{-9}

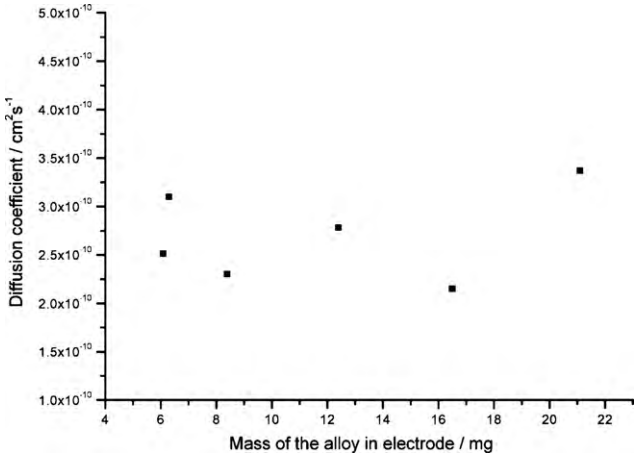

Fig. 10. Hydrogen diffusion coefficient, *D*, calculated from constant potential desorption experiments as a function of the active mass of AB_5 alloy. *SOC* = 100%, chronoamperometric measurements.

diffusion coefficient values determined for various electrodes and using various techniques (CA and CP) are in good agreement. On the other hand, the stability of the hydrogen capacity strongly depends on the method of the electrode preparation. The changes of the capacity recorded during cyclic charging/discharging process are connected with detachment of the active electrode material due to pulverisation of the hydrogen storage alloy. The observation of the presence of the alloy particles on the bottom of the electrochemical cell after the experiment confirms this suggestion. Although our electrode preparation method partly prohibits electrode degradation, only application of additional Teflon® holder allows reducing the capacity loss to only 9% of the nominal capacity.

Finally, we prepared a series of thin, Limited Volume Electrodes containing modified AB_5 hydrogen storage alloy with average particle size of ca. 4 μm. Fig. 11 shows the comparison of a constant current discharge capacity calculated for standard and modified AB_5 alloys in LV electrode at various temperatures.

One can note that at temperatures below −10 °C the capacity of the modified alloy is much higher than that of the standard one. Due to the peculiarities of binder free LV electrode construction we can conclude that the very high capacity recorded for modified alloy at −30 °C is connected only with the intrinsic properties of the alloy and is not related to the properties of binding agents or conductive materials which are simply absent in LVE. Further works on the modified alloy are in progress and the results will be reported in a separate communication.

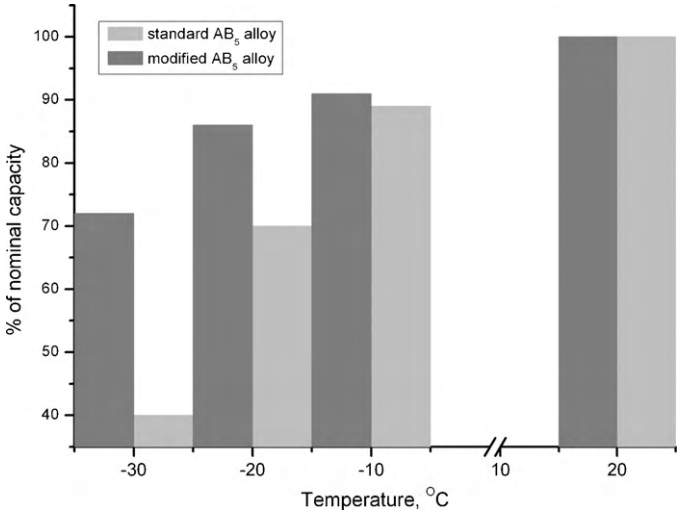

Fig. 11. A comparison of a constant current ($45\ mA\ g^{-1}$) discharge capacity calculated for LV electrodes containing standard and modified AB_5 alloy recorded at various temperatures. Before discharging the electrodes were fully charged ($60\ mA\ g^{-1}$) at room temperature.

4. Conclusions

The presented results show that a stable (up to twenty cycles of charging/discharging) metal hydride alloy electrode with a small amount of the alloy and without binder additives can be prepared in a very simply way. The electrochemical behaviour (CV curves) of the new electrode is similar to that reported in the literature for electrodes containing a single particle of a metal alloy. In this case the new electrode acts as a "Limited Volume Electrode". The active material is located inside the holes of the metal mesh and does not cover the metal mesh wires so the thickness of the new electrode corresponds to the diameter of a single alloy particle. The decrease of the electrode capacity (up to 33% after 20 cycles) recorded during charging–discharging experiments is connected with active mass loss due to detachment of alloys' particles from the electrode. The metal alloy losses can be significantly diminished by putting the electrode in a special Teflon holder. A comparison of the results obtained for the standard AB_5 alloy with two average particle sizes of 50 and 4 μm shows that the latter possesses much better hydrogen capacitance at temperatures below −10 °C. Reduction of the alloy particle size facilitates the also activation process.

The demonstrated method of electrode preparation and investigation is very convenient for estimating the kinetic and transport parameters in the pure electrode material, i.e., those reflecting real metal hydride behaviour e.g. hydrogen diffusion coefficient. The knowledge about the kinetic and the thermodynamic parameters of processes occurring in the pure hydrogen absorbing alloys helps in the design and construction of new, efficient power sources.

Acknowledgements

This work was supported by the European Commission through HydroNanoPol (UE 032517) – a project of the 6th Framework Programme of the European Union awarded for the years 2006–2009, and by the Polish Ministry of Science and Higher Education through accompanying grant 340/6.PRUE/2007/7.

References

[1] D. Linden, T.B. Reddy, Handbook of Batteries, third ed., McGraw-Hill, New York, 2002.
[2] M.A. Fetcenko, S.R. Ovshinsky, B. Reichman, K. Young, C. Fierro, J. Koch, A. Zallen, W. Mays, T. Ouchi, J. Power Sources 165 (2007) 544–551.
[3] C. Pillot, Main trends for the rechargeable battery market worldwide 2007–2015, http://www.avicenne.com/gb/batteries_and_power_supply_publications.htm#articles_and_presentations.
[4] G. Zheng, B.S. Haran, B.n. Popov, R.E. White, J. Appl. Electrochem. 29 (1999) 361–369.
[5] M. Geng, D.O. Northwood, Int. J. Hydrogen Energy 21 (1996) 887–890.
[6] D. Yan, W. Cui, J. Alloys Compd. 293–295 (1999) 780–783.
[7] T. Ise, T. Murata, Y. Hirota, M. Nogami, S. Nakahori, J. Alloys Compd. 298 (2000) 310–318.
[8] D.M. Kim, H. Lee, K. Cho, J.Y. Lee, J. Alloys Compd. 282 (1999) 261–267.
[9] K. Naito, T. Matsunami, K. Okuno, M. Matsuoka, C. Iwakura, J. Appl. Electrochem. 23 (1993) 1051.
[10] M. Geng, J. Han, F. Feng, D.O. Northwood, Int. J. Hydrogen Energy (1998) 1055.
[11] A. Zuttel, F. Meli, L. Schapbach, J. Alloys Compd. 221 (1995) 207–211.
[12] P.D. Vidts, J. Delgado, R.E. White, J. Electrochem. Soc. 142 (1995) 4006.
[13] J.M. Heikonen, H.J. Ploehn, R.E. White, J. Electrochem. Soc. 145 (1998) 1840.
[14] P.H.L. Notten, M. Ouwerkerk, H. van Hal, D. Beelen, W. Keurb, J. Zhoua, H. Feil, J. Power Sources 129 (2004) 45–54.
[15] B. Sakintunaa, F. Lamari-Darkrimb, M. Hirscherc, Int. J. Hydrogen Energy 32 (2007) 1121–1140.
[16] D.M. Borsa, R. Gremaud, A. Baldi, H. Schreuders, J.H. Rector, B. Kooi, P. Vermeulen, P.H.L. Notten, B. Dam, R. Griessen, Phys. Rev. B 75 (2007) 205408.
[17] S. Løken, J.K. Solberg, J.P. Maehlen, R.V. Denys, M.V. Lototsky, B.P. Tarasov, V.A. Yartys, J. Alloys Compd. 446–447 (2007) 114–120.
[18] A. Czerwiński, I. Kiersztyn, M. Grdeń, J. Czapla, J. Electroanal. Chem. 471 (1999) 190–195.
[19] A. Czerwiński, I. Kiersztyn, M. Grdeń, J. Electroanal. Chem. 492 (2000) 128–136.
[20] A. Czerwiński, Electrochim. Acta 39 (1994) 431–436.
[21] H.S. Kim, M. Nishizawa, I. Uchida, Electrochim. Acta 45 (1999) 483–488.
[22] A.J. Bard, L. Faulkner, Electrochemical Methods. Fundamentals and Applications, Wiley, New York, 1980.
[23] Yuan, N. Xu, J. Appl. Electrochem. 31 (2001) 1033.
[24] X. Tuan, N. Xu, J. Alloys Compd. 316 (2001) 113–117.
[25] J. Chen, S.X. Dou, D.H. Bradhurst, H.K. Liu, Int. J. Hydrogen Energy 23 (1998) 177–182.
[26] S. Majorowski, B. Baranowski, J. Phys. Chem. Solids 43 (1982) 1119.
[27] E. Wicke, H. Brodowsky, Top. Appl. Phys. 29 (1978) 73.
[28] F. Feng, D.O. Northwood, J. Power Sources 136 (2004) 346.